PV Module Energy Rating Standard IEC 61853-3 Intercomparison and Best Practice Guidelines for Implementation and Validation

Ruben Vogt, Malte; Riechelmann, Stefan; Gracia-Amillo, Ana Maria; Driesse, Anton; Kokka, Alexander; Maham, Kinza; Karha, Petri; Kenny, Robert; Schinke, Carsten; More Authors

Important note
To cite this publication, please use the final published version (if applicable).
Please check the document version above.

PV module energy rating standard IEC 61853-3 intercomparison and best practice guidelines for implementation and validation

M. R. Vogt[1,13,+,*], S. Riechelmann[2,+], A. M. Gracia-Amillo[3,+], A. Driesse[4,+], A. Kokka[5], K. Maham[5], P. Kärhä[5], R. Kenny[3], C. Schinke[6,1], K. Bothe[1], J. C. Blakesley[8], E. Music[2,7], F. Plag[2], G. Friesen[9], G. Corbellini[9], N. Riedel-Lyngskær[10], R. Valckenborg[11], M. Schweiger[12], W. Herrmann[12]

[*]Corresponding author: m.r.vogt@tudelft.nl
[+]Member of the taskforce for analyzing the results and investigating the inconsistencies
[1]Institute for Solar Energy Research Hamelin (ISFH), Am Ohrberg 1, 31860 Emmerthal, Germany
[2]Physikalisch-Technische Bundesanstalt (PTB), Bundesallee 100, 38116 Braunschweig, Germany
[3]European Commission, Joint Research Centre (JRC), Via E. Fermi 2749, Ispra, Italy
[4]PV Performance Labs, Freiburg, Germany
[5]Aalto University, Metrology Research Institute, Maarintie 8, 02150 Espoo, Finland
[6]Institute for Solid State Physics, Leibniz University Hannover (LUH), Appelstr. 2, 30167 Hannover, Germany
[7]Institut za mjeriteljstvo Bosne i Hercegovine (IMBiH), Augusta Brauna 2, BA-71000 Sarajevo, Bosnia and Herzegovina
[8]National Physical Laboratory (NPL), Hampton Road, Teddington. TW11 0LW. UK
[9]University of Applied Sciences and Arts of Southern Switzerland, SUPSI-PVLab, 6850 Mendrisio, Switzerland
[10]Technical University of Denmark (DTU), Dept. of Photonics Engineering, Roskilde, Denmark
[11]TNO, High Tech Campus 21, Eindhoven, The Netherlands
[12]TÜV Rheinland Energy GmbH, 51101 Cologne, Germany
[13]Now with: Delft University of Technology, PVMD, Mekelweg 4, 2628CD Delft, The Netherlands

Abstract— The IEC 61853 standard series aims to provide a standardized measure for PV module energy rating, namely the Climate Specific Energy Rating (CSER). For this purpose, it defines procedures for the experimental determination of input data and algorithms for calculating the CSER. However, some steps leave room for interpretation regarding the specific implementation. To analyze the impact of these ambiguities, the comparability of results and the clarity of the algorithm for calculating the CSER in part 3 of the standard, an intercomparison is performed among research organizations with 10 different implementations of the algorithm. We share the same input data, obtained by measurement of a commercial crystalline silicon PV module, among the participating organizations. Each participant then uses their individual implementations of the algorithm to calculate the resulting CSER values. The initial blind comparison reveals differences of 0.133 (14.7%) in CSER. After several comparison phases, a best practice approach is defined, which reduces the difference by a factor of 210 to below 0.001 (0.1%) in CSER for two independent PV modules. The best practice presented in this paper establishes clear guidelines for the numerical treatment of the spectral correction and power matrix extrapolation, where the methods in the standard are not clearly defined. Additionally, we provide input data and results for the PV community to test their implementations of the standard's algorithm. To identify the source of the deviations, we introduce a climate data diagnostic set. Based on our experiences, we give recommendations for the future development of the standard.

Index Terms—Energy rating, Energy yield, Energy Performance, PV module.

I. INTRODUCTION

The IEC 61853 standard series "Photovoltaic (PV) module performance testing and energy rating" was completed in 2018 with the publication of parts 3 and 4 [1], [2]. This followed the publication of part 1 dealing with power rating and part 2 dealing with incidence angle effects and module operating temperature, in 2011 and 2016 respectively [3], [4]. The series aims to provide a standardized measure for PV module performance, namely the Climate Specific Energy Rating (CSER), which is calculated in Part 3.

It is important to distinguish between the two related but different concepts of energy yield prediction and energy rating, since they have two very different objectives. Energy yield prediction is an estimate of the energy produced by a particular PV system constructed

in a particular way in a particular location. It typically needs at least 10 years of location specific data in order to consider site specific climatic characteristics as well as intra and inter-annual climatological variability. The energy yield estimation requires taking into consideration many parameters, including the specific location and mounting conditions, the local environment and climate. Energy rating is a simplified measure of how a given module type will tend to perform in different climates. It can be estimated based on one single year of data and it allows a quantitative comparison between module types. The energy rating datasets and methods are not intended to predict energy yield at any particular location.

For the purpose of energy rating, 6 reference climate datasets[5] describing the most representative working conditions that PV installations worldwide are subjected to are specified in Part 4 of the standard. The CSER relates the module energy efficiency in the reference climates to the module power efficiency under Standard Testing Conditions (STC: 25°C, 1000 Wm⁻², AM1.5G) [6] and thus aims to be a practical measure of performance in real conditions. The detailed procedure for the calculation of CSER is contained in Part 3, using input data from the other three parts. Part 3 contains 20 equations additionally the user has to derive another 18 equations to cover all extrapolation possibilities surrounding the power matrix. Thus many calculation steps are required and the specific implementation of the calculation is left to the user, and some steps in the procedure may be subject to different interpretations. Both of these factors mean that there is a risk that different CSER results may be obtained by different laboratories and institutions. Without a reference parameter set available to the PV community, it is impossible to verify the correctness of the implementation of the CSER calculation.

This work reports comparisons of CSER calculation implementations at ten different institutions. Different programming languages were employed including Python, Matlab and JSL. At least one participant provides the code in open source [7]. Significant differences in results were found in the first intercomparison round [8], demonstrating that even for experienced users, the standard is not straightforward to implement. Five intercomparison rounds were needed to resolve issues, ranging from programming bugs to interpretation difficulties. These intercomparison rounds culminated in a robust implementation and very close results for all participants, when tested on an independent module dataset. It was found that the spectral correction and extrapolation of module power are the two calculation steps that cause the most issues with interpretation of the standard. The former can be traced back to the standard not defining the exact procedure and method for numerical integration and for dealing with different spectral resolutions in the spectral correction step. The later can be traced back to the standard not defining the exact procedure and method for extrapolation of the module power or rather efficiency table for some cases.

In order to establish best practice guidelines for the PV community, the detailed steps and potential pitfalls are described, as well as the reasoning behind the interpretation considered most appropriate where some ambiguity of calculation steps is found.

A reference parameter set is provided, which will allow users to test their implementation and compare their results with those of this group. The dataset includes a complete definition of all the module parameters needed (measured as defined in parts 1 and 2 of the standard series), as well as the resulting CSER values for the 6 climate profiles. To aid debugging of implementations, a climate data diagnostic set is also provided which contains a small number of hourly data from part 4 of the standard series, chosen to highlight specific issues, along with appropriate intermediate output data.

Finally, the intensive work performing the intercomparisons involving all 4 parts of the standard series have enabled identification several areas for possible improvements. Some recommendations are made, which focus on the calculation steps in part 3, but since all 4 parts are closely related, it is advantageous to ensure any proposed changes are made in a consistent manner in all 4 parts.

A. IEC 61853 standard series overview

The IEC 61853 Standard series "Photovoltaic (PV) module performance testing and energy rating" establishes requirements for determining PV module performance in terms of power (watts), specific module energy rating (kWh/kW) and Climate Specific Energy Rating (dimensionless). The methodology does not take into account either progressive degradation or transient behaviour such as light induced changes and/or thermal annealing. The standard presently applies to mono-facial modules only. No other technologies are explicitly excluded, so it is possible to rate PV modules with all type of absorber materials and cell architectures. The standard series consists of the following four parts:

IEC 61853 Part 1 "Irradiance and temperature performance measurements and power rating" describes requirements for evaluating PV module performance in terms of power (watts) rating over a range of irradiances from 100 to 1100 Wm⁻² and module temperatures from 15°C to 75°C. This part is used to determine the so-called power matrix, which is

one of the main input data required in the calculation methods applied in Part 3.

IEC 61853 Part 2 "Spectral responsivity, incidence angle and module operating temperature measurements" describes test procedures to obtain the effect of varying angle of incidence (AOI) between the received irradiance and the module's surface and sunlight spectra content (i.e. spectral responsivity) on the effectively absorbed irradiance. The angular-loss (a_r) coefficient is extracted from the AOI test data, which is based on the Martin and Ruiz model [9], [10]. The higher the a_r coefficient, the greater the angular-dependent losses. Part 2 also describes the experimental procedures to obtain the u_0 and u_1 thermal coefficients that are required to estimate the module temperature $T_{mod,j}$ from in-plane irradiance $G_{corr,AOI,j}$, ambient temperature $T_{amb,j}$ and wind speed v_j. The u_0 and u_1 coefficients are from the Faiman model [11], and describe the effect of radiation and wind cooling on module temperature, respectively.

IEC 61853 Part 3 "Energy rating of PV modules" describes the calculation steps needed for PV module ratings. The input data to these calculations include the measurements and parameters obtained in parts 1 and 2, and the meteorological conditions available in part 4. The calculation steps are shown schematically in figure 1.

IEC 61853-4 Part 4 "Standard reference climatic profiles" contains six standard reference climatic profiles describing the most representative working conditions of PV installations worldwide. The six Standard Reference Climatic Profiles are subtropical arid (sub. ari.), subtropical coastal (sub. cos.), tropical humid (tro. hum.), temperate continental (tem. con.), temperate coastal (tem. cos.) and high elevation (hig. ele.). The mounting condition is defined to be a free standing fixed rack, equator facing and with an inclination angle β which is fixed at 20˚. Each dataset contains 8760 hourly values of several climatological variables over a year, including irradiance, ambient temperature and wind speed. A number of irradiance parameters are provided: horizontal, in-plane global and direct broadband irradiance, as well as in-plane spectrally resolved global irradiance from 307 nm to 4606 nm integrated in 29 discrete bands[12].

B. Calculating CSER

For each of the 6 reference climatic profiles, the calculations steps in part 3 are as follows:

The first step of the calculation algorithm is correcting the in-plane beam B_j and sky diffuse D_j irradiation for angular losses at the PV module interface due to oblique angle of incidence θ_j. For this purpose, the model of Martin and Ruiz [9], [10] is used (eqn. 1 & 2), based on the angular loss coefficient a_r of the PV module. Please note, that we use the same equation numbers as the 2018 version of the IEC 61853-3 standard to simplify comparison and add letters to the equation numbers, if we introduce modified versions.

The second step is spectral correction [4] of the angular corrected irradiance $G_{corr,AOI,j} = B_{corr,j} + D_{corr,j}$ for the mismatch between the spectrally resolved global irradiance given in the climate data set and AM1.5G reference spectrum [13]. The result is the corrected global irradiance $G_{corr,j}$, for which we propose eqn. 5a.

The third step is the calculation of the module temperature $T_{mod,j}$, for which the Faiman model is used [11] (eqn. 8).

$$B_{corr,j} = B_j \left[\frac{1 - \exp\left(-\frac{\cos(\theta_j)}{a_r} \right)}{1 - \exp\left(-\frac{1}{a_r} \right)} \right] \quad (1)$$

$$D_{corr,j} = D_j \left\{ 1 - \exp\left[-\frac{1}{a_r} \left(\frac{4}{3\pi} \left(\sin\beta + \frac{\pi - \beta - \sin\beta}{1 + \cos\beta} \right) + (0.5a_r - 0.154) \left(\sin\beta + \frac{\pi - \beta - \sin\beta}{1 + \cos\beta} \right)^2 \right) \right] \right\} \quad (2)$$

$$T_{mod,j} = T_{amb,j} + \frac{G_{corr,AOI,j}}{u_0 + u_1 v_j} \quad (8)$$

The fourth step is the calculation of the module power output for the given hour. For this purpose, the module power is measured according to [3] at different module temperatures (15-75°C) and irradiances (100-1100 Wm^{-2}). These results form a power matrix consisting of 22 power values, converted to module efficiency through dividing by irradiance. Two-dimensional bilinear interpolation is then used to determine the module efficiency at the corrected global irradiance $G_{corr,j}$ and the module temperature $T_{mod,j}$ values. Afterward, the obtained module efficiency value is used to calculate power output $P_{mod,j}$ for the given hour j and the process (Steps 1-4) is repeated for every hour of the year. The energy produced by the module is the sum of the hourly values. The CSER is then calculated using equation 20,

$$CSER = \frac{E_{mod,year} / H_{p,year}}{P_{max,STC} / G_{ref,STC}}, \quad (20)$$

Module input

1. Angular loss a_r
2. Spectral response
3. Thermal co. u_0, u_1
4. Power matrix

Climate input

1. Sun angle, in-plane direct and global irradiance
2. Spectrally resolved global in-plane irradiance
3. Ambient Temperature T_{amb}

1. Angular correction of irradiance $G_{corr,AOI,j}$ (1-2)

2. Spectral corrected irradiance $G_{corr,j}$ (5a)

3. Module temperature $T_{mod,j}$ (8)

4. Calculation of the module power $P_{mod,j}$ (9-17c)

While j < 8760

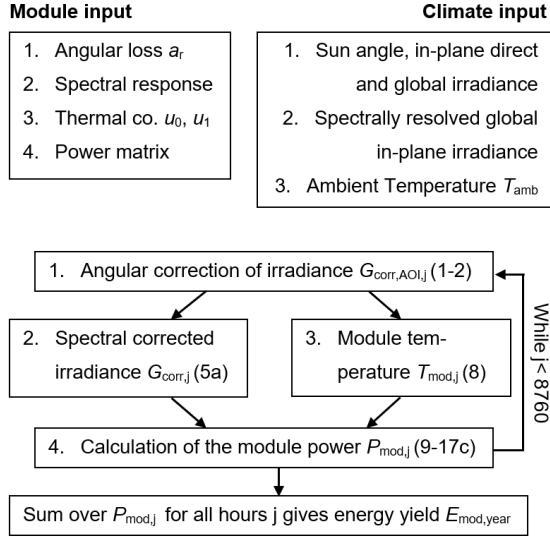Sum over $P_{mod,j}$ for all hours j gives energy yield $E_{mod,year}$

Figure 1: Main steps and input parameters for each step of the IEC61853-3 algorithm and the equation number in this work.

Where $E_{mod,year}$ is the total energy produced, relative to the total yearly irradiation in the module plane $H_{p,year}$ and the module's maximum power under STC $P_{max,STC}$ and the irradiance of the reference spectrum $G_{ref,STC}$. The CSER may be interpreted as the annual efficiency in the climate relative to STC efficiency, or as a PV module performance ratio (MPR) [5], [14]–[17]. A CSER of 1 means that the PV module operates as efficient in the climate as under STC, while CSER values below 1 indicate lower efficiency in the reference climate and vice versa.

II. TEST MODULE INPUT DATA

The Module 1 data set uses the thermal coefficients u_0=25 W/(m²×K) and u_1=6.84 W/(m³×s×K) taken from literature [11]. All other module parameters are measured at TÜV Rheinland, the results are in Tab. 1 and Fig. 2 in this work. All the module data is available in csv format in Appendix B – Input data module 1 and Appendix C – Input data module 2 of this paper as well as for download from https://www.metro-pv.ptb.de/home/. A standard c-Si module with 60 cells is used as the test module 1. A Pulsed solar simulator, class AAA according to IEC 60904-9 [18] is used to measure the power matrix according to IEC 61853-1 [3]. The results are shown in Table 1, listing the $P_{max,STC}$ value as 280.47 W. The spectral responsivity (as shown in Fig. 2, bottom) is measured according to IEC 61853-2 using a monochromator system with bias light source. A pulsed solar simulator, class AAA according to IEC 60904-9, is used for the incidence angle modifier (IAM) measurement according to IEC61853-2. The measured values are the black symbols in Fig. 2 top. In the first phase of the

intercomparison campaign participants determined their own a_r angular loss coefficient by fitting the measurement data themselves using different fitting methods. This lead to deviations up to 0.008 in a_r. As this study is focused on part 3 of the series and not part 2, it was decided to use the $a_r = 0.14571$ (black line Fig. 2 left) for all other phases.

TABLE I
MODULE POWER [W] FOR MODULE 1 AT THE SPECIFIED TEMPERATURES AND IRRADIANCES IN IEC 61853-1 MEASURED FOR THIS STUDY.

Intensity [W/m²]	Temperature [°C]			
	15°C	25°C	50°C	75°C
100	26.60	25.77	NA	NA
200	56.04	53.80	NA	NA
400	114.89	110.46	99.24	NA
600	174.09	167.57	150.84	133.80
800	232.89	224.16	202.05	179.35
1000	291.36	280.47	252.45	224.08
1100	NA	308.05	277.36	246.06

TABLE II
MODULE POWER [W] FOR MODULE 2 AT THE SPECIFIED TEMPERATURES AND IRRADIANCES IN IEC 61853-1 TAKEN FROM [19].

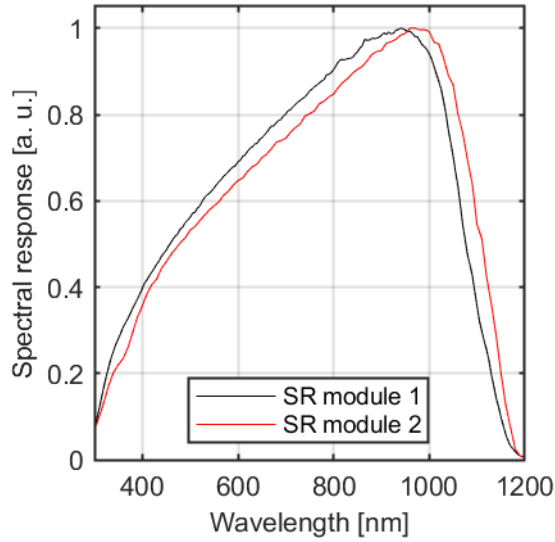| Intensity [W/m²]	Temperature [°C]			
	15°C	25°C	50°C	75°C
100	28.83	27.71	NA	NA
200	59.26	57.01	NA	NA
400	120.65	115.95	104.72	NA
600	182.0	175.04	157.86	140.13
800	242.05	233.19	209.93	186.43
1000	301.23	289.88	260.73	231.39
1100	NA	317.58	285.20	253.47
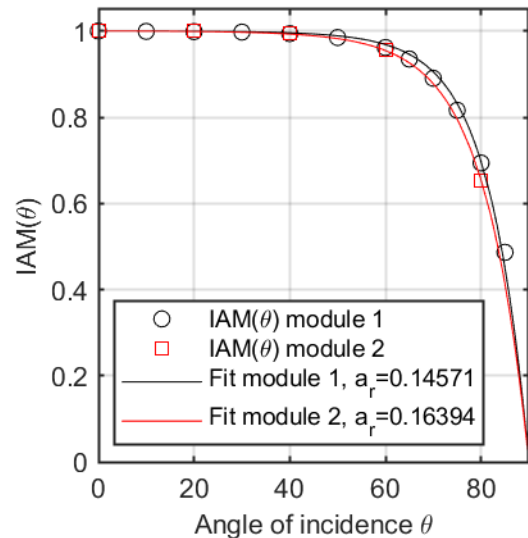
Figure 2: Incidence angle modifier (top) and spectral responsivity (bottom) of the two modules used in the intercomparison campaign. Please note, that the values for module 1 are measured, while the values for module 2 are obtained via simulation.

Since no complete set of PV module input parameters for IEC 61853-3 was available in literature, input parameters from different literature sources all describing c-Si modules are combined to form a second data set. This collection of PV module input parameters will be referred to as "module 2", to simplify descriptions. The Module 2 data set uses the thermal coefficients u_0=26.4 W/(m²×K) and u_1=6.25 W/(m³×s×K) taken from literature [11]. The module power matrix as shown in Table 2 is taken from [19]. The spectral response and angular behavior of module 2 are simulated using the Daidalos cloud ray tracer [20], which demonstrated good agreement with measurements in several studies [21]–[24]. The results are shown in red in Figure 2.

III. INTERCOMPARISON RESULTS

In the first phase of the intercomparison [8], each participant calculated the results for module 1 without knowledge of the other participants' results. The results from phase 1 are shown in Fig. 3 for all six climate profiles. The largest difference between two participants was 0.133 (14.7%) in the tropical humid profile, but even the high elevation climate with the lowest difference of 6.7% still showed a significant deviation. Please note, that result J1 was excluded due to the use of input parameters from a different module and that the star next to participant F in phase 5 signifies that two dimensional inter- and extrapolation functions build into a python software package are used rather than the explicit equations given in Appendix A. Also note that the results including
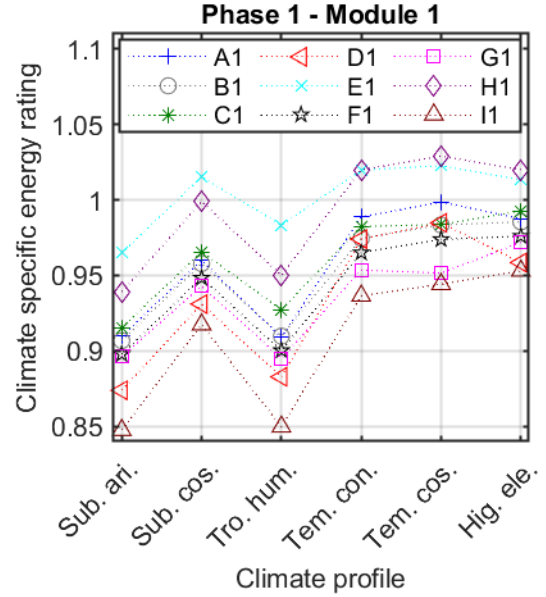
Figure 3: Climate specific energy ratings for all participants and climate profiles for the same module in the initial blind comparison.

The results of the final comparison round (Phase 5, Fig. 4) show a difference of 0.00066 (0.07%) in CSER for the temperate continental climate and less in all other climate profiles (down to 0.00018 (0.02%) in CSER for the subtropical arid climate profile).
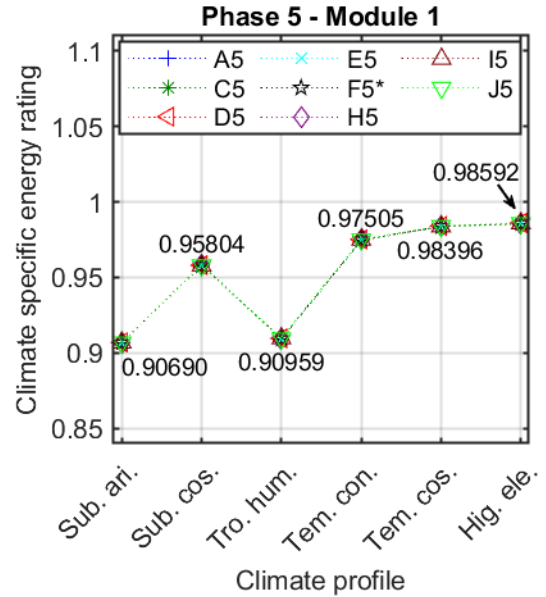

Figure 4: Climate specific energy ratings for all participants and climate profiles for the same module in the final comparison round. The median of all participants' values is the respective number shown for each climate.

Figure 5 shows the development of the largest relative difference between any two participants for

each climate profile through all five phases. This difference declines from 14.7% in phase 1, to 3.2% in both phases 2 and 3, to 1.2% in phase 4 and down to 0.07% in phase 5. This is a reduction by a factor of 210 between of the highest relative difference in phase 1 and 5. The relative differences shown in Fig. 5 are defined by the two most disagreeing participants, if we discard the results for the half of the participants, which are furthest from the median: We would get a difference of 4.8% in phase 1, to 0.33% in phase 2, to 0.20% in phase 3, to 0.022% in phase 4 and down to 0.0042% in phase 5. This is an even greater reduction (factor of 1152) for the core results surrounding the median of each phase. Signifying that the improvements are achieved by all participants. Please, note that participants B and G stopped contributing results in phase 4 and 5 due to other work priorities, the deviation of their phase 3 results from the final median CSER is 0.21% or less for all climate profiles.
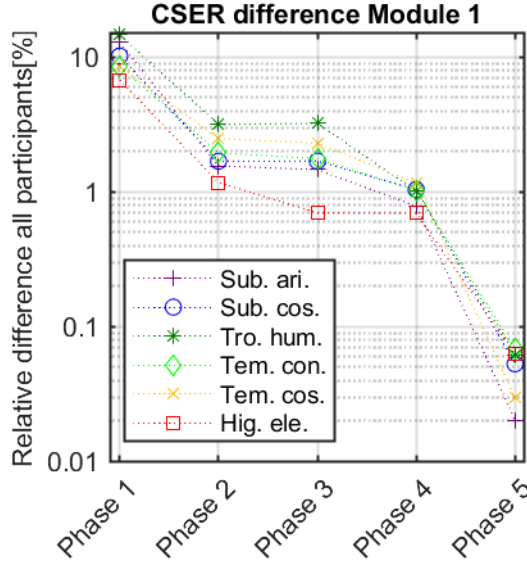

Figure 5: The largest relative difference between any two participants for module 1 in each climate and phase declines from 14.7% to 0.07%.

IV. BEST PRACTICE

During the intercomparison, we identified three main sources for errors [8], namely the AOI correction based on the determination of a_r values from angle of incidence measurements, the spectral correction of in-plane irradiance and the determination of instantaneous module power through inter- and extrapolation. In the following, we present additional guidance in interpreting the standard in a way that will provide consistent results.

A. Recommendations for the AOI correction procedure

The correction of angle of incidence effects requires

the a_r factor, that represents the angular responsivity of the device under test. In IEC 61853-2, it is described, that this factor has to be determined by "an appropriate fitting procedure". We here recommend to use a least square fit optimization with measurement data and to limit to the range from 0° to 80° incidence angle. Measurements of higher incidence angles are increasingly prone to systematic measurement errors and therefore measurements at 85° should be rejected[24]. In the CSER calculation, the angular loss coefficient should be specified with an accuracy of five digits to prevent the impact of the fitting and rounding on the calculation.

B. Recommendations for the spectral calculation of in-plane irradiance

The spectral correction is based on spectrally resolved global irradiance data given in the IEC 61853-4 and is performed by Eqn. 5, 6 and 7 of IEC 61853-3. In our analysis of the spectral correction [8], we noticed that this step is a main source for the deviations. One of the origin for that is that the spectral correction factor, defined by Eqn. 6 of IEC 61853-3, does not give the value of 1, if one corrects with the reference spectrum R_{STC}. Several participants rectified this by replacing the 1000 with their value for $\int_{\lambda_s}^{\lambda_e} R_{STC}(\lambda) \cdot d\lambda$. By substituting Eqn. 7 to Eqn. 6 we eliminate the spectral correction factor and thus a deviation source and derive:

$$G_{corr,j} = 1000 \cdot \frac{\int_{\lambda_s}^{\lambda_e} S(\lambda) \cdot R_{corr,AOI,j}(\lambda) \cdot d\lambda}{\int_{\lambda_s}^{\lambda_e} S(\lambda) \cdot R_{STC}(\lambda) \cdot d\lambda} \quad , \qquad (5a)$$

Another origin of the spectral deviation are the steps and limits of the numerical integration. While the standard states, that the integration limits are $\lambda_s = 300$ nm and $\lambda_e = 4\,000$ nm, the spectrally resolved global irradiance data in part 4 is given in 29 so-called Kato bands [12], ranging from 306.8 nm to 4605.65 nm. In addition, the spectral responsivity $S(\lambda)$ and the spectral intensity of the AM1.5 spectrum have different resolutions compared to the Kato bands. We suggest to perform the following steps to harmonize the input data and solve equation 5a:

1. To get $S(\lambda)$ to the Kato grid, first use linear interpolation to add data points to the existing grid at the wavelength edges of the corresponding Kato band. If for example the initial wavelength grid of your $S(\lambda)$ is $\lambda = 300, 305, 310, 315, 320, 325, 330, \dots 1200$ nm, then perform a linear interpolation to $\lambda = 306.8, 310, 315, 320, 325, 327.8$ nm.

2. Apply the trapezoidal rule for numerical integration with the now extended wavelength grid to derive an $S(\lambda)$ value corresponding to the first Kato waveband.

3. Repeat 1 and 2 until you have values for 28 Kato bands. Some of these bands will have an value of zero, since $S(\lambda)$ is 0 beyond 1200 nm. <u>Kato band 29 is skipped.</u>

4. <u>Repeat Steps 1-3 for $R_{STC}(\lambda)$. Again, only 28 Kato bands are calculated, since the last Kato band ranges from 3991 nm to 4605.65 nm, where the AM1.5 standard spectrum is not defined.</u>

5. <u>Now</u> $S(\lambda)$, $R_{STC}(\lambda)$ and $R_{corr,AOI,j}(\lambda)$ all have exactly 28 values, corresponding to the Kato bands. Use them as an input in the for equation 5 and calculate the products in the integrals.

6. Now just sum up the values in the integrals and multiply with 1000 to derive $G_{corr,j}$.

C. Recommendations for the determination of instantaneous module power

For the determination of instantaneous module power, the standard recommends converting the power matrix to an efficiency matrix. To determine efficiency at arbitrary irradiance and temperature levels defined by the working conditions using 2-D bilinear interpolation, or equivalent is recommended. In the round-robin the focus remained on the bilinear approach and alternative methods were not investigated. A recent report on bilinear and alternative methods points out that for a typical PV efficiency matrix, bilinearly interpolated values will always be underestimated and extrapolated values will always be overestimated [25]. Other PV-specific methods are available that would reproduce the module efficiency characteristics with greater accuracy, and would also be suitable for the energy rating task [26]. However, allowing different methods could introduce a bias in CSER related to the method, therefore it is more important to agree on a single method even if is perhaps not the best.

Bilinear interpolation is a well-known method whereby an interpolation in two dimensions is made by performing linear interpolation along one dimension, followed by a linear interpolation along the other dimension. The order in which this is done does not affect the interpolated value. Extrapolation is done by changing one or both of the linear interpolation steps into linear extrapolation from the nearest grid points. Normally a bilinear interpolation or extrapolation calculation requires four distinct known points on the rectangular grid formed by the two dimensions, in this case temperature and irradiance. Unfortunately, around the irregular perimeter of the power/efficiency matrix, it is not obvious everywhere which known points (measured temperatures and irradiances) should be used for the extrapolation. Thus, some additional guidance is required to avoid inconsistent results.

Firstly, not all extrapolation equations needed for deriving P(G,T) are formulated explicitly in the

standard. A visual overview of the various interpolation and extrapolation cases occurring when $P(G,T)$ is derived from the G-T matrix is given in figure 6. The standard provides the Equations 9-11 for interpolation of $P(G,T)$ values inside the range of the G-T matrix. For extrapolating $P(G,T)$, the Equations 12-14 are given in the standard if 100 W/m² < G < 1100 W/m² and T > 75 °C. If both G > 1100 W/m² and T > 75 °C, Equations 15-17 of the standard shall be applied. All other extrapolation equations, e.g. for G < 100 W/m², have to be derived from the given equations, which is prone to errors. Therefore, we added all formulas necessary for extrapolation of irradiance and temperature to Appendix A. Note that variations of the standard equations are marked by an extra letter, e.g. 14a for an extrapolation for $P(G,T)$ with G < 100 W/m². For easier reading we use the same equation numbers (9-17) as in the standard.

	< 15 °C	15 °C	25 °C	50 °C	75 °C	> 75 °C
> 1100 W/m²	15c-17c	12c-14c	12c-14c	12c-14c		15-17
1100 W/m²	12b-14b	?	9-11	9-11		12-14
1000 W/m²	12b-14b	9-11	9-11	9-11		12-14
800 W/m²	12b-14b	9-11	9-11	9-11		12-14
600 W/m²	12b-14b	9-11	9-11	?		12-14
400 W/m²	12b-14b	9-11	?	?		12-14
200 W/m²	12b-14b	9-11	?	?		12-14
100 W/m²	15b-17b	12a-14a	12a-14a	12a-14a		15a-17a

Legend:
- ● G-T matrix values
- ● missing matrix values
- ▢ interpolation (Eqns. in standard)
- ▢ extrapolation (Eqns. in standard)
- ▢ extrapolation (Eqns. have to be derived)
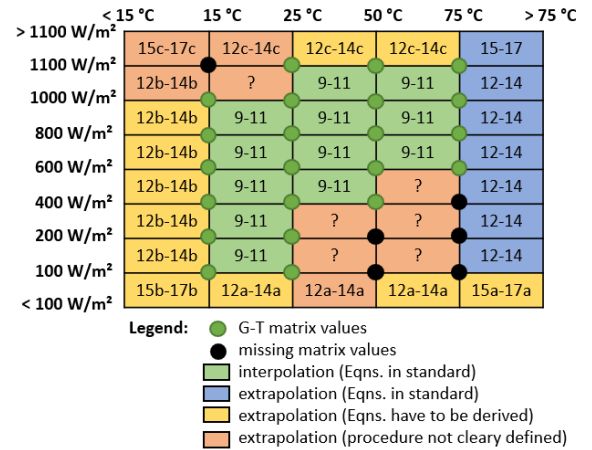- ▢ extrapolation (procedure not cleary defined)

Figure 6: Visualization of all inter- and extrapolation regions of the G-T-matrix used to derive P(G,T) in the IEC 61853-3 standard. Annotations in the boxes specify the equations needed for deriving P(G,T) values here. Question marks signal the possibility of ambiguous solutions.

Secondly, missing G-T matrix values lead to ambiguous extrapolations. A total of six data points of the G-T matrix are left blank to reduce measurement effort in IEC 61853-1. In this case a $P(G,T)$ data point has three known neighbors. It is not specified which equation is applicable for this case. Possible options are an extrapolation along the temperature axis by applying Equations 12-14, an extrapolation along the irradiance axis by applying Equations 12a-14a, or a flat plane extrapolation with Equations 15a-17a. Before starting the determination of P(G,T), we recommend to fill up missing measurements in the matrix. Of the three possible options, linear extrapolation along the irradiance axis produced the least plausible efficiency values, whereas extrapolation along the flat plane formed by the nearest known grid points produced the most realistic trends. For simplicity, however, it is recommended to use the third option, which is linear

extrapolation along the temperature axis with Eqn. 14b when T = 15 °C and with Eqn. 14 when T >= 50 °C, respectively (Fig. 7).
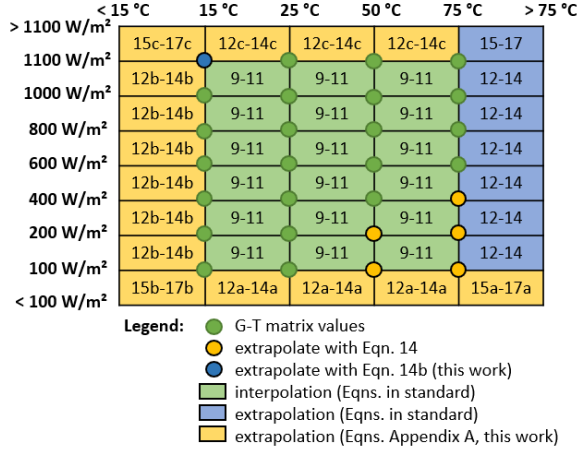

Figure 7: Visualization of our approach to derive P(G,T) based on equations of the IEC 61853-3 standard. Before P(G,T) can be extrapolated, the missing data values in the G-T matrix are filled up with Formula 14 of the standard and its deviation Formula 14a, respectively.

V. VERIFICATION WITH INDEPENDENT MODULE DATA

In order to verify that the improved agreement is not only limited to module 1, another blind comparison round is conducted with a new module (module 2). As in the initial blind comparison, the participants calculated the CSER values without the knowledge of the other participants' results.

The results are shown in Fig. 8. The highest difference among all participants for module 2 is 0.00091 (0.095%) in CSER for the subtropical coastal profile and less in all other climate profiles down to 0.00044 (0.044%) in CSER for the high elevation climate profile. In conclusion, a deviation of less than 0.1% between the different implementations is maintained for all climate profiles, which is significantly lower than the typical measurement uncertainty for the input parameters.
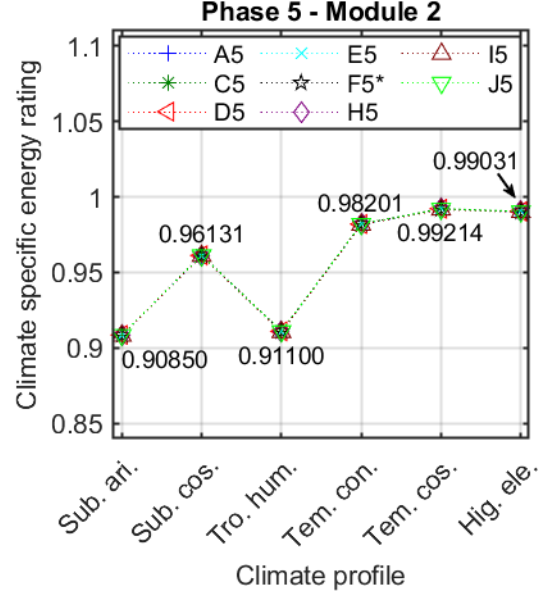

Figure 8: The median of all participants' values is the respective number shown for each climate. The highest difference among all participants for module 2 is 0.00091 (0.095%) in CSER. This verifies, in another blind comparison round, that the improvements in agreement achieved are reproducible with other modules.

VI. CLIMATE DATA DIAGNOSTIC SET

During the intercomparison, we recognized the need to easily identify the source of differences in the CSER calculation. To achieve this purpose, the climate data diagnostic set given in Appendix D is created. It has the same format as the climate data given in part 4 of the standard, but just 96 rows instead of 8760. Additionally, the climate data is artificially created for testing five different aspects of the CSER algorithm:

1. The first aspect tested is the treatment of direct and diffuse irradiation. This is done by the data in Appendix D row 1-6 (month 1), where the direct fraction of the irradiation is increased from 0 to 100%.

2. The second aspect tested is the treatment of different incidence angles. This is done by the data in Appendix D row 7-16 (month 2), where the angles of incidence is increased from 0° to 90°.

3. The third aspect tested is the treatment of different spectral bands. This is done by the data in Appendix D row 17-45 (month 3), where all irradiance is concentrated in one band scanning through all 29 individually bands row by row.

4. The next aspect tested is the temperature behavior. This is done by the data in Appendix D row 46-56 (month 4), where the wind speed is increased from 0 to 10 m/s.

5. The last aspect tested is the module power with respect to whole temperature as well as irradiance range. This is done by the data in Appendix D row 57-96 (month 5). The artificial climate data forces the algorithm to calculate the module power for each field in Figures 6 and 7 from top left to bottom right, thus

covering all inter- and extrapolation scenarios. Even some, which are non-existent in the climate data of part 4.

When using the climate data diagnostic set, the best practice approach with the respective module input data we calculate a CSER of 0.86528 for module 1 and 0.86644 for module 2 or within 0.1% of this value. As discussed in section III, at least half of the participants are within 0.005% of these values, thus we recommend to aim for an agreement in this range. The hourly results for AOI corrected irradiation, spectral correct irradiation, module temperature and power for each hour/row are given in Appendix E and F .

VII. SUMMARY AND CONCLUSION

The practical implementation of IEC 61853-3 is more complicated than one might expect as demonstrated by the initial comparison with differences of 0.133 (14.7%) in CSER. However, after several comparison phases, a best practice approach is defined, which reduces the difference in CSER to below 0.001 (0.1%) for two independent modules.

The best practice approach establishes clear guidelines for the numerical treatment of the spectral correction and power matrix extrapolation, where the standard is not clearly defined. According to the best practice approach, the spectral correction step should use the 28 Kato bands between 306.8 nm and 3991 nm. In the spectral correction term, linear interpolation should be performed to generate points at band edges. Afterwards, the trapezoidal rule should be used for integration. For the power matrix extrapolation, explicit equations are given in Appendix A for all possible combinations of temperature and irradiance.

The climate data diagnostic set introduced in this paper is created to identify the source of the following deviations: Differences in the treatment of direct and diffuse irradiation as well as their angular correction, testing the module temperature based on wind as well as irradiation changes, comparing the spectral correction for each Kato band individually and revealing differences in the inter- or extrapolation in any of the 40 regions inside as well as surrounding the power matrix points.

For future versions of the IEC 61853-3 standard, we recommend that all calculation steps are clearly defined by equations for all cases, integration limits and numerical methods. However, from a software development perspective, the use of build-in software functions for certain tasks such as interpolation should be allowed. Of course there is a wide range of software development packages with built in functions, thus it should be tested on a case by case basis that the used function is comparable to the explicit equation in the standard. In addition to the guidelines established in this work for part 3, the mathematical fit algorithm for determining the angular loss coefficient should be defined by future versions of 61853-2. We here recommend to use a least square fit optimization with measurement data limited to the incidence angle range from 0° to 80° and that angular loss coefficient should be specified with an accuracy of five digits to reduce the impact of the fitting and rounding in CSER calculation.

REFERENCES

[1] "IEC61853-3: PV module performance testing and energy rating - Part 3: Energy rating of PV modules." 2018.

[2] "IEC61853-4: PV module performance testing and energy rating - Part 4: Standard reference climatic profiles." 2018.

[3] "IEC61853-1: PV module performance testing and energy rating - Part 1: Irradiance and temperature performance measurements and power rating." 2011.

[4] "IEC61853-2: PV module performance testing and energy rating - Part 2: Spectral responsivity, incidence angle and module operating temperature measurements." 2016.

[5] T. Huld, E. Salis, A. Pozza, W. Herrmann, and H. Müllejans, "Photovoltaic energy rating data sets for Europe," *Solar Energy*, vol. 133, pp. 349–362, Aug. 2016, doi: 10.1016/j.solener.2016.03.071.

[6] "IEC61836: Solar photovoltaic energy systems - Terms, definitions and symbols." 2016.

[7] A. Driesse, *PV Performance Labs Tools for Python*. https://github.com/adriesse/pvpltools-python, 2020. [Online]. Available: https://github.com/adriesse/pvpltools-python

[8] M. R. Vogt *et al.*, "Interlaboratory comparison of the PV module energy rating standard IEC 61853-3," EUPVSEC 2020, pp. 811–816.

[9] N. Martin and J. M. Ruiz, "Calculation of the PV modules angular losses under field conditions by means of an analytical model," *Sol. Energy Mater. Sol. Cells*, no. 70, pp. 25–38, 2001.

[10] N. Martin and J. M. Ruiz, "Corrigendum to Calculation of the PV modules angular losses under field conditions by means of an analytical model," *Sol. Energy Mater. Sol. Cells*, 2012, [Online]. Available: http://dx.doi.org/10.1016/j.solmat.2012.11.002

[11] D. Faiman, "Assessing the outdoor operating temperature of photovoltaic modules," *Prog. Photovolt: Res. Appl.*, vol. 16, no. 4, pp. 307–315, Jun. 2008, doi: 10.1002/pip.813.

[12] S. Kato, T. P. Ackerman, J. H. Mather, and E. E. Clothiaux, "The k-distribution method and correlated-k approximation for a shortwave radiative transfer model," *Journal of Quantitative Spectroscopy and Radiative Transfer*, vol. 62, no. 1, pp. 109–121, May 1999, doi: 10.1016/S0022-4073(98)00075-2.

[13] "IEC 60904-3: Photovoltaic devices - Part 3: Measurement principles for terrestrial photovoltaic (PV) solar devices with reference spectral irradiance data." 2019.

[14] D. Dirnberger, B. Müller, and C. Reise, "PV module energy rating: opportunities and limitations: PV module energy rating:

opportunities and limitations," *Prog. Photovolt: Res. Appl.*, vol. 23, no. 12, pp. 1754–1770, Dec. 2015, doi: 10.1002/pip.2618.

[15] M. Schweiger, "Performance of PV Modules with Different Technologies and the Impact on Energy Yield in Four Climatic Zones," Dissertation, Technischen Hochschule Aachen, 2017.

[16] J. C. Blakesley *et al.*, "Accuracy, cost and sensitivity analysis of PV energy rating," *Solar Energy*, vol. 203, pp. 91–100, Jun. 2020, doi: 10.1016/j.solener.2020.03.088.

[17] J. Bonilla Castro and M. Schweiger, "Climatic Rating of Photovoltaic Modules: Different Technologies for Various Operating Conditions," 2021.

[18] "IEC60904-9: Photovoltaic devices - Part 9: Solar simulator performance requirements." 2007.

[19] CFV Labs, "19074 PAN File Report: Hanwha Q CELLS Q.Peak-G4.1 300 Module," Dec. 2019. [Online]. Available: https://pvpmc.sandia.gov/pv-research/pv-lifetime-project/pv-lifetime-modules/

[20] M. R. Vogt *et al.*, "Boosting PV Module Efficiency beyond the Efficiency of its Solar Cells – A Ray Tracing study with DAIDALOS now available to the Scientific Community," *EUPVSEC 2019*, pp. 795–800.

[21] H. Holst *et al.*, "Application of a New Ray Tracing Framework to the Analysis of Extended Regions in Si Solar Cell Modules," *Energy Procedia*, vol. 38, pp. 86–93, 2013, doi: 10.1016/j.egypro.2013.07.253.

[22] H. Holst *et al.*, "Increased Light Harvesting by Structured Cell Interconnection Ribbons: An Optical Ray Tracing Study Using a Realistic Daylight Model," *Energy Procedia*, vol. 92, pp. 505–514, Aug. 2016, doi: 10.1016/j.egypro.2016.07.134.

[23] M. Köntges, H. Schulte-Huxel, S. Blankemeyer, M. R. Vogt, H. Holst, and R. Reineke-Koch, "Measuring the light recovery factor of backsheets in photovoltaic modules," *Solar Energy Materials and Solar Cells*, vol. 186, pp. 175–183, Nov. 2018, doi: 10.1016/j.solmat.2018.06.028.

[24] N. Riedel-Lyngskær and A. A. Santamaría Lancia, "Interlaboratory comparison of angular-dependent photovoltaic device measurements: Results and impact on energy rating," *Progress in Photovoltaics: Research and Applications*, vol. 29, no. 3, pp. 315–333, doi: 10.1002/pip.3365.

[25] A. Driesse and J. Stein, "From IEC 61853 power measurements to PV system simulations.," 2020. [Online]. Available: https://www.osti.gov/biblio/1615179

[26] A. Driesse, M. Theristis, and J. S. Stein, "A New Photovoltaic Module Efficiency Model for Energy Prediction and Rating," *IEEE J. Photovoltaics*, vol. 11, no. 2, pp. 527–534, Mar. 2021, doi: 10.1109/JPHOTOV.2020.3045677.